POLITECNICO
MILANO 1863

SCUOLA DI INGEGNERIA INDUSTRIALE
E DELL'INFORMAZIONE

Executive Summary of the Thesis

Quantum Well Infrared Photodetectors for Free Space Quantum Communications

Laurea Magistrale in Engineering Physics - Ingegneria Fisica

Author: Fabrice Monasterio — **24114**

Advisor: Prof. Andrea Crespi

Co-advisors: Dr. Baptiste Chomet, Prof. Carlo Sirtori

Academic year: 2024-2025

1. Introduction

The spectral bands of 3–5 µm, in Mid-Wavelength Infrared (MWIR), and 8–14 µm, in Long-Wavelength Infrared (LWIR), are particularly promising for free-space optical (FSO) quantum communications since they are the transparency windows for the atmosphere. Quantum Key Distribution (QKD) protocols based on continuous-variable (CV) [1] encoding of quantum information in the quadratures of coherent states of light are well suited for FSO links. CV-QKD manipulates the amplitude and phase quadratures of the optical field and therefore requires quadrature modulators together with high-efficiency, low-noise coherent detection schemes, such as heterodyne or balanced detection [2]. In particular, heterodyne detection is crucial for CV-QKD because it enables simultaneous access to both field quadratures, which direct detection cannot provide.
The development of robust and efficient LWIR coherent sources and detectors is crucial to fully unlock the potential of FSO quantum communications in the LWIR region. Sources must exhibit narrow intrinsic linewidths to ensure phase coherence over the duration of the quantum communication and prevent phase diffusion. Detectors must provide low noise characteristics, high bandwidths, and elevated saturation powers to handle strong local oscillator fields.
This thesis addresses these challenges by focusing on two complementary aspects. The first is a characterization of the frequency noise of a distributed feedback (DFB) quantum cascade laser (QCL) using heterodyne detection with a quaternary metamaterial quantum well infrared photodetector (QWIP). This demonstrates the capability of QWIPs to serve as heterodyne detectors while simultaneously enabling measurement of the intrinsic linewidth of the DFB-QCL source. The second aspect is the intensity noise characterization of a second DFB-QCL together with a comprehensive noise analysis and modelling of the QWIP detector.

1.1. Quaternary Metamaterial QWIP

The QWIP used in this work is based on a quaternary metamaterial architecture, InGaAs/InAlAs for the barrier material and InGaAs for the quantum wells (QWs). The active region consists of $N_{\mathrm{QW}} = 13$ periods of alternating QW and barrier grown perpendicular to the device plane. The use of the quaternary alloy allows lattice matching with the InP sub-

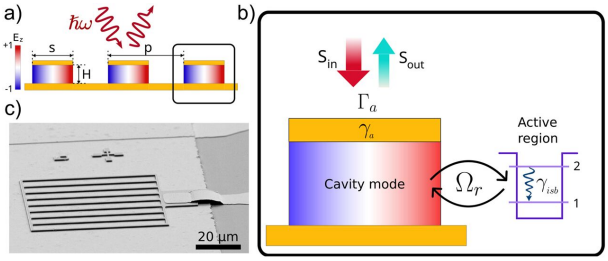

Figure 1: a) Geometry of array stripes. b) Coupling mode theory representation of the system. c) SEM image of a stripe array device. From [3].

strate, which is advantageous for monolithic integration of optoelectronic components in photonic integrated circuits (PIC).
The metamaterial architecture is based on a metal-dielectric-metal (MDM) cavity [4] arranged in a stripe array configuration (fig. 1c) [3] to reduce the electrical area while maintaining a large optical area (antenna effect). The stripe geometry (fig. 1a) can be engineered to tune the absorption wavelength of the QWIP. The MDM cavity (fig. 1b) couples the incident light to the QWs, enhancing the light-matter interaction and improving device performances. The cavity mode ensures that the polarization selection rule for intersubband transitions (ISBT) is satisfied for normally incident light.

2. Frequency Noise Characterization

2.1. Key Theory and Definitions

The intrinsic linewidth of a laser is fundamentally limited by spontaneous emission in the laser cavity [5]. A semiclassical description was first provided by Schawlow and Townes in 1958. After adapting the original formula to account for phase-amplitude coupling in semiconductor lasers, the Schawlow–Townes linewidth expression becomes:

$$\Delta\nu_{\mathrm{ST}} = \frac{h\nu_{\mathrm{L}}}{2\pi\tau_{\mathrm{c}}^2 P_{\mathrm{out}}}(1+\alpha_{\mathrm{LEF}}^2), \qquad (1)$$

where $h\nu_{\mathrm{L}}$ is the photon energy, τ_{c} the photon decay time ($\Delta\nu_{\mathrm{c}} = 1/2\pi\tau_{\mathrm{c}}$ is the resonator bandwidth), P_{out} the optical output power and α_{LEF} the linewidth enhancement factor. The formula represents a fundamental lower bound for the linewidth of a continuous-wave laser and shows that the linewidth narrows with increasing optical power.

Heterodyne detection is essential for measuring the frequency noise of lasers, as it allows for the extraction of phase information from the beatnote generated by mixing the source laser with a stable reference beam (local oscillator). The beating signal describes the interference pattern created by the two electromagnetic fields:

$$S(t) \propto \cos\Big(\Delta\omega t + \delta\varphi_{\mathrm{S}}(t)\Big), \qquad (2)$$

where $\Delta\omega$ is the difference in angular frequency between the source and the reference laser and $\delta\varphi_{\mathrm{S}}(t)$ is the phase fluctuation of the signal. In deriving eq. (2), the assumption that the phase fluctuations of the reference laser are negligible ($\delta\varphi_{\mathrm{REF}}(t) \approx 0$) is made, which allows focusing solely on the phase noise of the signal $\delta\varphi_{\mathrm{S}}(t)$.

2.2. Methods

A heterodyne detection scheme was implemented to measure the frequency noise of a DFB-QCL. The laser source under test was mixed, using a beam splitter, with a strong reference laser impinging on a biased QWIP detector. The resulting beatnote, with a typical frequency of hundreds of megahertz, was amplified and digitized. The time-domain signal was analyzed and processed using the analytical signal formalism, crucial for extracting the instantaneous phase. A phase noise power spectral density (PNPSD) $S_\varphi(f)$, in rad^2/Hz, was computed from the phase time series and allowed for the extraction of the frequency noise PSD (FNPSD) $S_\nu(f)$, in Hz^2/Hz, using the relation $S_\nu(f) = f^2 S_\varphi(f)$ which can be derived from $\nu = (1/2\pi)\,\mathrm{d}\varphi/\mathrm{d}t$.
The measured frequency-noise power spectral density white plateau S_ν^{white}, in units of Hz^2/Hz, is directly related to the Schawlow–Townes linewidth, expressed in Hz, by $\Delta\nu_{\mathrm{ST}} = \pi S_\nu^{\mathrm{white}}$. A measurement of the plateau frequency as a function of optical power thus allows the extraction of several cavity parameters such as τ_{c}, $\Delta\nu_{\mathrm{c}}$, and the quality factor Q.
The PNPSD $S_\varphi(f)$ is formed by three distinct regions: at low frequencies it exhibits technical noise contributions ($1/f^\gamma$ noise), at intermediate frequencies it follows a $1/f^2$ trend characteristic of white frequency noise and finally at high frequencies it exhibits a white plateau whose level is directly proportional to the signal-to-noise ratio (SNR) of the measured beatnote. The

FNPSD $S_\nu(f)$ thus exhibits a $1/f^{\gamma-2}$ technical noise region at low frequencies, a flat (white) region S_ν^{white} corresponding to the Schawlow–Townes plateau, and a high-frequency f^2 trend due to the finite SNR. To observe the Schawlow–Townes linewidth, it is essential to minimize the technical noise of the reference laser and achieve a high SNR in the heterodyne beatnote.

As illustrated in the lower part of fig. 2, to reduce the technical noise the reference laser *REF* was stabilized by phase-locking it, via a phase-locking loop (PLL), to an ultra-stable Optical Frequency Comb Synthesizer (OFCS) to form a powerful local oscillator that inherits the low phase noise characteristics of the OFCS. The use of a QWIP as a heterodyne detector allows high SNR detection due to its elevated saturation power, enabling the use of powerful local oscillators, which makes it possible to observe the Schawlow–Townes plateau.

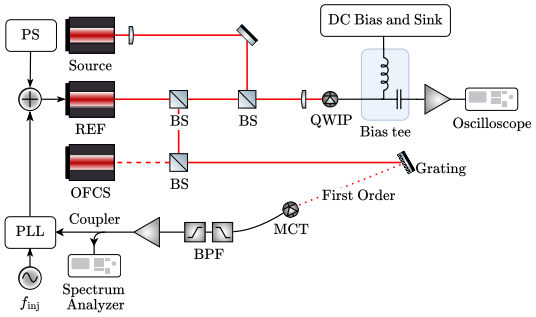

Figure 2: Heterodyne detection setup and phase-locking of the reference laser.

2.3. Results

The heterodyne beatnotes achieved a SNR of approximately 55 dB, enabling precise extraction of frequency noise. The wavelength of the lasers was 9.31 µm. A representative FNPSD is shown in fig. 3 and was measured with the source laser operating at 14.6 mW. A fit of the low- and high-frequency regions trends are displayed along with their sum, representing the noise floor of the measurement. The white plateau is clearly visible above the noise floor, confirming the ability to measure the intrinsic linewidth. Taking the difference between the white plateau S_ν^{white}, visible between 3 MHz and 5 MHz, and the noise floor S_ν^{floor} yields $\Delta\nu_{\text{ST}}(14.6\,\text{mW}) = \pi(S_\nu^{\text{white}} - S_\nu^{\text{floor}}) = 603\,\text{Hz}$.

The noisy region that follows the plateau, visible between 7 MHz and 10 MHz, is intrinsic to

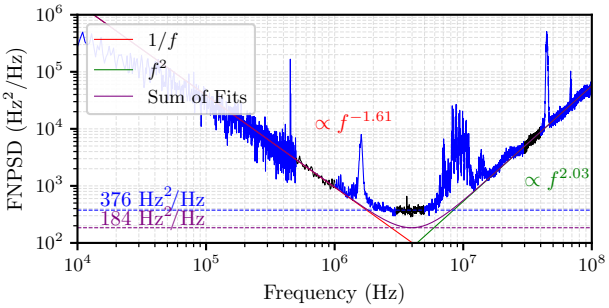

Figure 3: Measured frequency-noise PSD of the QCL showing the Schawlow–Townes plateau.

the reference laser, and analysis highlighted the presence of two spurious signals with repeating frequencies, one at ≈ 40 kHz and the second at 1 kHz. These signals are likely related to the Peltier element (TEC) used to stabilize the laser temperature.

To demonstrate the independence of the plateau frequency, namely of the Schawlow–Townes linewidth, on the optical power of the reference laser, two sets of measurements were performed varying the power of reference laser by several tens of milliwatts while keeping the source laser power constant at 6.1 mW for the first one and 20.5 mW for the second one. The dependence of the emitted wavelength on the operating optical power set a limit to the maximum power that could be used for the local oscillator without losing the beatnote. In both experiments, the Schawlow–Townes linewidth showed no significant dependence on the reference laser power, confirming that the measured linewidth is the one of the source laser.

Conversely, to demonstrate the dependence of the Schawlow–Townes linewidth on the optical power of the DFB-QCL under analysis, several beatnotes were acquired varying the source laser power while adapting the reference laser power to obtain the highest possible SNR. This tuning was performed by slightly changing the temperature of the reference laser and the injection current to match the wavelength of the source laser and obtain a beating at a frequency within the detection bandwidth of the QWIP. The results are plotted in fig. 4, which depicts the dependence of the plateau frequency on the inverse of the optical power. A linear fit of the data points represented in blue was constrained to pass through the origin. Measurements at higher optical powers, represented in black, were ex-

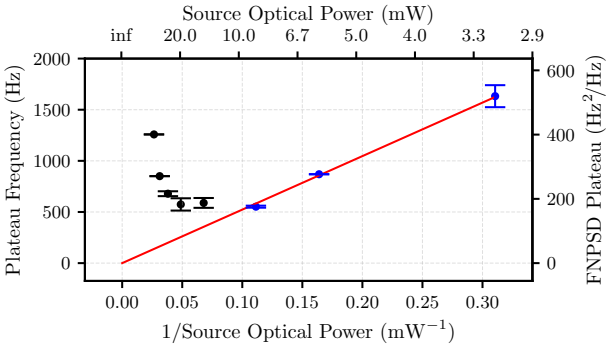

Figure 4: Dependence of the white frequency-noise plateau on inverse optical power.

cluded from the fit since they were affected by significant rollover effects characteristic of QCLs operating at high injection currents.
From the slope of the linear fit and eq. (1), several cavity parameters were extracted. The photon decay time was found to be $\tau_c = 18\,\text{ps}$, corresponding to a cavity bandwidth $\Delta\nu_c = 8.8\,\text{GHz}$ and a quality factor $Q = 3645$.

3. Intensity Noise Characterization

3.1. Key Theory and Definitions

The relative intensity noise (RIN) quantifies the normalized power fluctuation spectrum $\delta P^2(f)$ (one-sided PSD, in W^2/Hz) of a light source:

$$\text{RIN}(f) = \delta P^2(f)/P_0^2. \tag{3}$$

For QWIPs [6], the photocurrent is given by:

$$I_{\text{ph}} = e\,\Phi\,\eta\,g_{\text{ph}} = P_0\,\mathcal{R} = (h\nu\Phi)\,\mathcal{R}, \tag{4}$$

where e is the electron charge, Φ is the photon flux, η is the quantum efficiency associated with the intersubband absorption, g_{ph} is the photoconductive gain, P_0 is the incident optical power, $h\nu$ is the photon energy and $\mathcal{R}$ is the responsivity.
The capture and escape probabilities, p_c and p_e, respectively, describe the dynamics of electron interactions in the active region:

$$p_{\text{c}} = \frac{\tau_{\text{trans}}}{\tau_{\text{c}} + \tau_{\text{trans}}}, \quad p_{\text{e}} = \frac{\tau_{\text{relax}}}{\tau_{\text{esc}} + \tau_{\text{relax}}}, \tag{5}$$

where τ_{trans} is the electron transition time over a single QW, τ_{c} is the capture time (lifetime of the excited electron), τ_{esc} is the escape time from the well, and τ_{relax} is the intersubband relaxation time.
The dark current gain g_{noise} and the photoconductive gain g_{ph} are defined as:

$$g_{\text{noise}} = \frac{1}{N_{\text{QW}}\,p_{\text{c}}}, \quad g_{\text{ph}} = \frac{p_{\text{e}}}{N_{\text{QW}}\,p_{\text{c}}}, \tag{6}$$

where N_{QW} is the number of quantum wells in the QWIP structure.
The associated dark current and photocurrent noise densities, in A^2/Hz, are:

$$i^2_{\text{dark}} = 4e\,g_{\text{noise}}\,I_{\text{dark}}, \tag{7}$$

$$i^2_{\text{ph}} = 4e\,g_{\text{ph}}\,I_{\text{ph}}. \tag{8}$$

In the detector, two additional noise contributions are present, the first from the source laser $i^2_{\text{s}} = \text{RIN}\,I^2_{\text{ph}}$ and the second from the thermal noise $i^2_{\text{th, QWIP}}$ associated with the detector differential resistance R_{QWIP} and temperature T_{QWIP}.
The detection chain adds two further noise sources that can be independently calculated: the thermal noise of the equivalent input resistance $i^2_{\text{th, }50\,\Omega}$ (in parallel with R_{QWIP}) and the amplifier noise i^2_{amp}.
Finally, the total measured current noise PSD is:

$$i^2_{\text{tot}} = i^2_{\text{th, QWIP}} + i^2_{\text{dark}} + i^2_{\text{ph}} + i^2_{\text{s}} + i^2_{\text{th, }50\,\Omega} + i^2_{\text{amp}}. \tag{9}$$

The conversion between current noise PSD i^2 and voltage noise PSD v^2 must consider the equivalent resistance $R_{50\,\Omega} \parallel R_{\text{QWIP}}$.
In QWIPs, the total current noise does not necessarily scale linearly with the impinging optical power, as predicted by eq. (8), due to changes in R_{QWIP} that affect the thermal noise contribution. Hence, to extract i^2_{ph}, a full noise analysis is required.

3.2. Methods

The laser RIN was measured using a Mercury-Cadmium-Telluride (MCT) photodetector in direct detection. The beam optical power was varied by changing the injection current to change the working conditions. After amplification, the photocurrent was analyzed in the frequency domain using an Electronic Spectrum Analyzer (ESA). The RIN was calculated from the ratio between the mean-square optical-noise term

$\delta P^2(f)$, in W^2/Hz, and the square of the average optical power P_0^2, in W^2. This allows for the calculation of the RIN for any Fourier frequency f within the detection bandwidth. Confidence intervals were determined by requiring the illuminated signal to be above the dark noise floor by some multiple of the standard deviation of the latter. For DFB-QCLs, the RIN is expected to decrease with increasing optical power following an inverse power law.

To study the QWIP noise characteristics, the DFB-QCL previously used as reference was now employed as a laser source. To study the dark current noise, the non-illuminated detector was biased at different voltages and the voltage noise PSD v_{tot}^2 was recorded. For the investigation of the noises in the illuminated QWIP, the impinging optical power was varied using two polarizers to keep the laser operating conditions constant. In both cases, the voltage noise PSD v_{tot}^2 was acquired and averaged in a frequency region where the noise is white.

Using the noise model previously described and eq. (9), the dark current noise i_{dark}^2 can be extracted from the total noise i_{tot}^2. Equation (7) then allows the calculation of the dark current noise gain g_{noise}. From g_{noise} and eq. (6), the capture probability p_c can be calculated. Finally, from p_c and an estimation of the transit time τ_{trans}, the capture time τ_c can be inferred. When the device is illuminated, eq. (8) allows the extraction of the photoconductive gain g_{ph} and from it the escape probability p_e can be calculated using eq. (6). Finally, using the value of i_{dark}^2 measured previously and eq. (9), the photocurrent noise i_{ph}^2 can be extracted.

3.3. Results

RIN values measured at several frequencies revealed the expected power dependence: the RIN follows an inverse power law $\text{RIN} \propto P^{-\gamma}$, where $\gamma \approx 2$. A representative RIN spectrum taken for a power of 10 mW is shown in fig. 5, along with three confidence intervals at 1σ, 2σ and 5σ. The noise peak at around 10 MHz is the same observed in the frequency noise measurements.

The analysis of the non-illuminated QWIP noise was accomplished by measuring the voltage noise PSD v_{tot}^2 and the differential resistance R_{QWIP} at different bias voltages making it possible to convert to current noise PSD i_{tot}^2. The

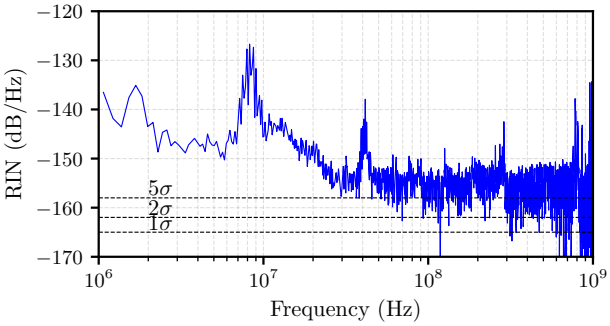

Figure 5: RIN at 10 mW.

bounds on the values for the bias voltage were imposed by the dark current magnitude. This allowed the calculation of the thermal noise contribution $i_{\text{th, QWIP}}^2$ and the extraction of the dark current noise i_{dark}^2 using eq. (9). The results are shown in fig. 6, where all noise sources are plotted and the overall noise, in blue, can be seen increasing exponentially with bias voltage. The total thermal noise $i_{\text{th, QWIP}}^2 + i_{\text{th, 50 Ω}}^2$ of the QWIP, in orange, depends on the differential resistance and thus is related to the bias voltage and the illumination power.

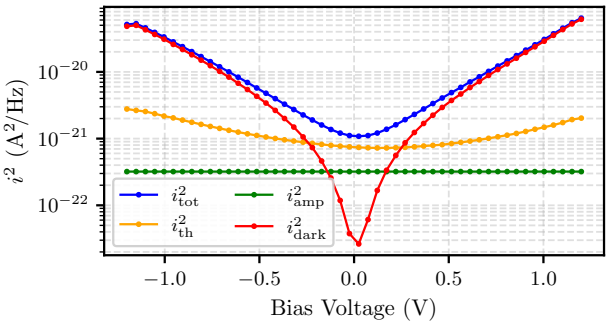

Figure 6: Current-noise PSD contributions in the non-illuminated QWIP.

The extracted dark current noise i_{dark}^2 was then used to calculate the dark current noise gain g_{noise}. Values greater than 1 for bias voltages exceeding 1 V were measured and could indicate possible electron-electron scattering phenomena under high electric fields. From g_{noise} and N_{QW}, the extracted capture probability p_c was calculated. The values of p_c exhibit the expected trend and exponential fits predict saturation values at approximately 5.6 % and 3.4 % for the negative and positive bias, respectively.

From the extracted capture probability p_c and an estimation of the transit time τ_{trans}, we inferred the capture time τ_c which was on the or-

der of 10 ps for a bias of 1.2 V, in agreement with literature values.
The analysis of the illuminated QWIP noise was carried out by first performing a bias sweep under constant illumination. This allowed the extraction of the responsivity $\mathcal{R}$ and the photoconductive gain g_{ph} as a function of bias voltage and both quantities increase with bias voltage. Secondly, the optical power was varied by two polarizers while keeping a fixed bias voltage of 1.2 V to study the dependence of the various noise contributions on the incident power. A responsivity of $\mathcal{R} = 0.35\,\mathrm{A/W}$ was measured at 1.2 V. From the measured voltage noise v_{tot}^2, the dark noise v_{dark}^2 was subtracted along with the other known noise sources to isolate the illuminated noise contributions $v_{\mathrm{ph}}^2 + v_{\mathrm{s}}^2$. Operating the DFB-QCL at high injection current reduced the RIN, as a result v_{s}^2 was negligible and v_{ph}^2 could be isolated. The expected linear dependence of the photocurrent noise i_{ph}^2 on the optical power could not be reliably observed due to inaccuracies in the differential resistance measurements under illumination influencing the thermal noise modelling.

4. Conclusions

This work demonstrated the suitability of quaternary metamaterial QWIPs to serve as ultrasensitive heterodyne detectors for LWIR free-space quantum communications. The characteristics of the QWIP detector, notably high saturation power and bandwidth, enabled coherent measurements with high SNR, allowing the observation of the intrinsic linewidth of a DFB-QCL via heterodyne detection. The measured Schawlow–Townes linewidths confirm the potential of QCLs for coherent communications as they imply a slow phase diffusion over time, which is crucial for maintaining coherence in CV-QKD.
The intensity noise analysis of both the DFB-QCL and the QWIP revealed favorable noise properties, with the DFB-QCL exhibiting low RIN at high powers and the QWIP demonstrating noise performance consistent with theoretical models. To achieve shot-noise-sensitive detection, further investigation is needed to more accurately model thermal noise under illumination and to reduce the dark current noise contribution.

Acknowledgements

I am grateful to Prof. Carlo Sirtori, Dr. Baptiste Chomet, Salim Basceken and the QUAD team for their support and guidance throughout this project carried out at the Laboratoire de Physique de l'École Normale Supérieure (LPENS) in Paris, France.
I also thank Prof. Andrea Crespi for his supervision and advices during the preparation of this thesis.

References

[1] E. Diamanti and A. Leverrier, "Distributing Secret Keys with Quantum Continuous Variables: Principle, Security and Implementations", Entropy **17**, 6072–6092 (2015).

[2] T. Gabbrielli et al., "Mid-infrared homodyne balanced detector for quantum light characterization", Optics Express **29**, 14536–14547 (2021).

[3] T. Bonazzi et al., "Metamaterial unipolar quantum optoelectronics for mid-infrared free-space optics", APL Photonics **9**, 110801 (2024).

[4] Y. Todorov et al., "Optical properties of metal-dielectric-metal microcavities in the THz frequency range", Optics Express **18**, 13886–13907 (2010).

[5] M. Pollnau and M. Eichhorn, "Spectral coherence, Part I: Passive-resonator linewidth, fundamental laser linewidth, and Schawlow-Townes approximation", Progress in Quantum Electronics **72**, 100255 (2020).

[6] H. Schneider and H. C. Liu, *Quantum Well Infrared Photodetectors*, Vol. 126, Springer Series in OPTICAL SCIENCES (Springer Berlin Heidelberg, 2006).